Future of Radionuclide Myocardial Perfusion Imaging: Transitioning from SPECT to PET

Marcelo F. Di Carli

Cardiovascular Imaging Program, Departments of Radiology and Medicine; Division of Nuclear Medicine and Molecular Imaging, Department of Radiology; and Division of Cardiovascular Medicine, Department of Medicine, Brigham and Women's Hospital, Harvard Medical School, Boston, Massachusetts

Over the past half century, radionuclide myocardial perfusion imaging (MPI) has played a transformative role in the evaluation of patients with suspected or known coronary artery disease (CAD). The quantification of the burden of myocardial ischemia and scarring has played a critical role in the diagnosis, risk prediction, and management of CAD. Meanwhile, there have been groundbreaking changes in competing testing options available for patients with suspected CAD. In addition, we have witnessed important changes in the epidemiology of CAD, which together with new scientific evidence are shaping the goals and choices of diagnostic imaging for CAD. This article reviews the pivotal role that radionuclide imaging has played in the management of patients with CAD and explores important changes to our radionuclide MPI practice that will be required to maintain and expand its transformative role in an era of multimodality imaging, with an emphasis on the necessary transition from SPECT to PET.

TRANSFORMATIVE ROLE OF RADIONUCLIDE MPI

Since its introduction in 1971 (*1*), the quantification of the extent and severity of reversible and irreversible perfusion defects has played a central role in the identification of obstructive CAD and the delineation of ischemic and scar burden that has been used as the basis for clinical decision-making regarding the potential need for coronary angiography and revascularization. A recognized strength of radionuclide MPI is its robust prognostic value that allows accurate risk-based management of CAD and forms the basis for its widespread use and clinical utility. The power of radionuclide MPI (including SPECT and PET) for risk stratification is based on the fact that major determinants of prognosis in patients with CAD are readily available from gated MPI. These include the amount of myocardial scarring and ischemia, left ventricular volumes and ejection fraction, coronary artery calcification (CAC) burden with hybrid imaging, and myocardial blood flow (MBF) and flow reserve measurements with PET. Optimal risk stratification is based on the concept that the risk associated with normal study results is sufficiently low that referral to revascularization will not further improve patient outcomes. Hence, catheterization is an unlikely option after testing. Conversely, patients with severely abnormal stress imaging results are at greater risk of adverse events and, thus, are potential candidates for intervention, and the magnitude of their risk is related to the extent and severity of the imaging abnormalities. The effectiveness of radionuclide MPI for risk stratification has been demonstrated for nearly all patient subsets (*2*,*3*). Although there is a strong separation between low- and high-risk patients across the clinical risk spectrum, event rates in patients with normal MPI but higher clinical or cardiac risk (e.g., diabetes mellitus (*4*) and chronic kidney disease (*5*)) are generally over 1%/y, suggesting that underlying clinical risk attenuates the effectiveness of risk reclassification after MPI, especially the identification of low-risk patients. As discussed below, this last observation has important implications because of the shift in referral patterns to radionuclide MPI from lower- to higher-risk patients, especially with the increased use of coronary CT angiography in lower-risk groups and the rise of cardiometabolic disease.

CHANGING EPIDEMIOLOGY AND CLINICAL PRESENTATION OF CAD: DOES IT MATTER?

Despite the undeniable clinical success of radionuclide MPI, there are signs that the epidemiology and clinical manifestations of CAD are changing and that the paradigm that served as the bedrock principle for the effectiveness of radionuclide MPI for many decades—that is, the search for obstructive CAD—may be insufficient to adequately evaluate patients with stable chest pain syndrome in modern cardiovascular medicine. Indeed, there is evidence that the frequency of obstructive CAD as a key driver of symptoms and clinical outcomes is declining. Over the last 2 decades, diagnostic yields for invasive coronary angiography (*6*–*9*) and noninvasive stress testing (*10*,*11*) have fallen in both men and women. At the same time, there has been a temporal decline in the incidence of acute presentations of ST-segment elevation myocardial infarction and a sharp increase in the rates of hospitalizations with a secondary myocardial infarction diagnosis and heart failure with preserved ejection fraction, associated with an increased prevalence of cardiometabolic risk factors (*12*,*13*). The rising epidemic of cardiometabolic disease (*14*) has been associated with an anatomic phenotype dominated by "diffuse atherosclerosis" and "microvascular remodeling" (*15*).

Cardiometabolic disorders represent a cluster of interrelated risk factors including hypertension, prediabetes and diabetes, obesity, and chronic kidney disease that are associated with an increased risk of adverse cardiovascular events. There is firm evidence that this cluster of comorbid conditions promotes a systemic proinflammatory state (*16*), which has been linked to adverse cardiac remodeling and

Received Aug. 24, 2023; revision accepted Oct. 5, 2023.
For correspondence or reprints, contact Marcelo F. Di Carli (mdicarli@bwh.harvard.edu).
Published online Nov. 1, 2023.

DOI: 10.2967/jnumed.122.264864

cardiovascular events, including heart failure (*17*). Increased systemic inflammation has been linked to endothelial dysfunction and coronary vasomotor abnormalities (*18*) that may play a central role in subclinical myocardial injury (elevated troponin levels) and subsequent diffuse interstitial fibrosis, increased myocardial strain (elevated N-terminal pro–b-type natriuretic peptide), increased left ventricular diastolic stiffness and systolic myocardial dysfunction, and ultimately adverse events, especially heart failure (*19–22*).

These changes help explain why the risk associated with a normal radionuclide MPI result has not necessarily been low (<1%) in higher-risk cohorts (e.g., patients who have diabetes or chronic kidney impairment or are elderly) (*4*,*5*,*23*), representing an increasing segment of the patients referred for radionuclide stress testing. The reasons for the observed increased adverse event rate in higher-risk cohorts despite a visually normal radionuclide MPI result are likely multifactorial. On one hand, clustering of comorbidities, including hypertension, obesity, diabetes, and other factors, increases clinical risk even in the absence of obstructive CAD. On the other hand, and notwithstanding the clinical utility of SPECT MPI, it is a somewhat insensitive test to uncover diffuse obstructive and nonobstructive CAD and coronary microvascular dysfunction (CMD) associated with myocardial ischemia and increased risk of adverse events. This is highlighted by a recent comparative effectiveness study assessing ischemic burden by SPECT and PET MPI in the same high-risk patients. Among patients with severe ischemia by PET, 41% had either no or mild ischemia when myocardial perfusion was measured via SPECT (Figs. 1 and 2). Conversely, among patients with severe ischemia on SPECT, 42% had less than severe ischemia on PET MPI (*24*). Furthermore, quantification of MBF with PET in patients with diabetes (*25*), hypertension (*20*,*22*), chronic kidney disease (*26*), and CAD (*27*) demonstrated a high frequency of abnormal coronary vasoreactivity and myocardial flow reserve in patients with normal and abnormal MPI, which was associated with a high risk of adverse outcomes, including heart failure, myocardial infarction, and death.

INTEGRATING MBF QUANTIFICATION INTO CLINICAL PET MPI

The shifting paradigm away from the dominant role of obstructive CAD presents formidable challenges for our traditional approach to CAD evaluation with radionuclide MPI. Quantification of MBF offers a powerful opportunity to tackle this challenge effectively. MBF (measured in mL/min/g of myocardium) and MBF reserve (MFR, defined as the ratio between stress and rest MBF) are important physiologic parameters that can be measured by routine postprocessing of myocardial perfusion PET images. These absolute measurements of MBF provide a measure of the integrated effects of focal coronary stenoses, diffuse atherosclerosis, and microvascular dysfunction on myocardial perfusion, and as such, the value obtained is a more sensitive and accurate measure of myocardial ischemia.

The integration of quantitative MBF and MFR information into scan interpretation improves detection of the extent and severity of

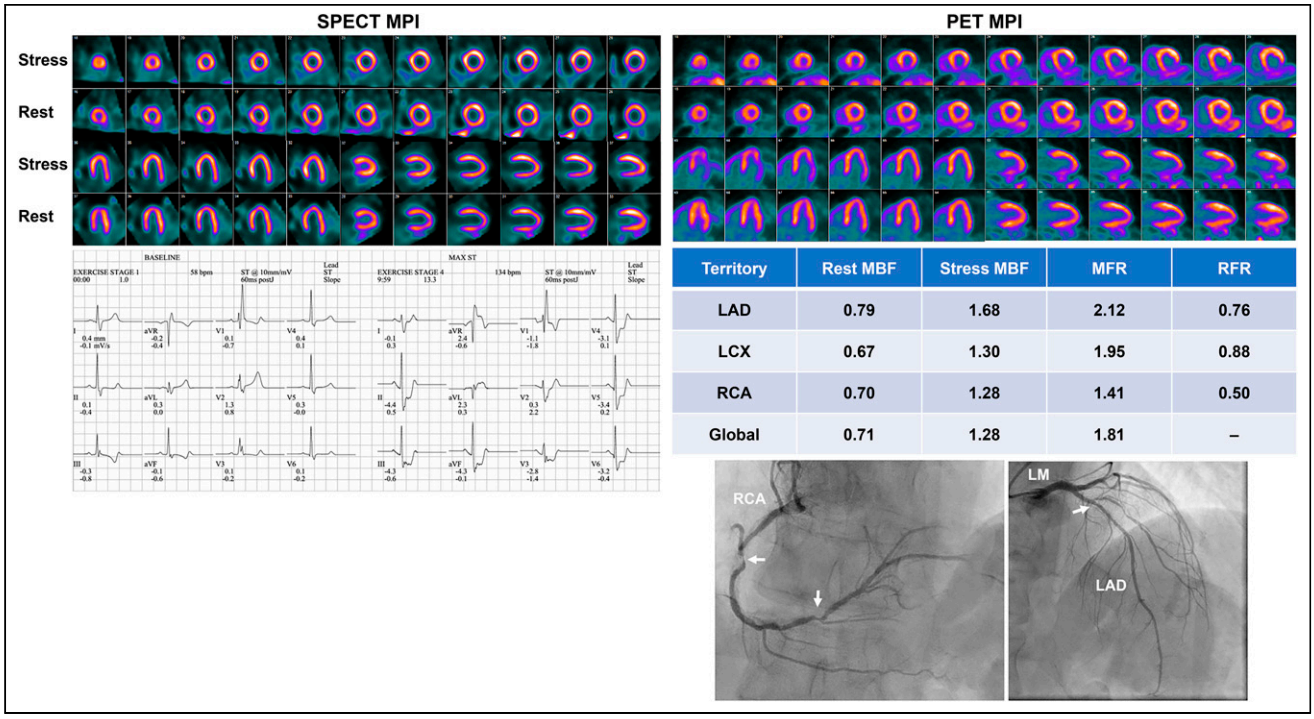

Territory	Rest MBF	Stress MBF	MFR	RFR
LAD	0.79	1.68	2.12	0.76
LCX	0.67	1.30	1.95	0.88
RCA	0.70	1.28	1.41	0.50
Global	0.71	1.28	1.81	–

FIGURE 1. Rest and stress SPECT and PET MPI images obtained 2 wk apart on 74-y-old man with known CAD and prior percutaneous coronary intervention presenting with recurrent chest pain. Patient initially underwent rest and stress SPECT MPI. He exercised for 10:00 min of Bruce protocol. His heart rate increased from 58 bpm at rest to peak of 134 bpm (92% of age-predicted maximal heart rate), and blood pressure increased from 130/64 mm Hg at rest to 148/62 mm Hg at peak exercise (rate–pressure product, 19,832). Patient developed chest pain and 2.5 mm of ST segment depression in leads II, III, aVF, and V3–V6, which resolved 11 min into recovery. SPECT images did not show significant perfusion defects. Patient was then referred for rest/stress PET MPI, which demonstrated large and severe perfusion defect throughout inferior and inferolateral walls with complete reversibility. This was associated with significant reduction in MFR in right coronary artery territory, associated with markedly reduced relative flow reserve. Coronary angiography showed 95% stenosis in mid right coronary artery and 70% stenosis in distal right coronary artery. There was 50% lesion in proximal left anterior descending coronary artery with normal instantaneous wave-free ratio. LAD = left anterior descending coronary artery; LCX = left circumflex coronary artery; LM = left main coronary artery; RCA = right coronary artery; RFR = relative flow reserve.

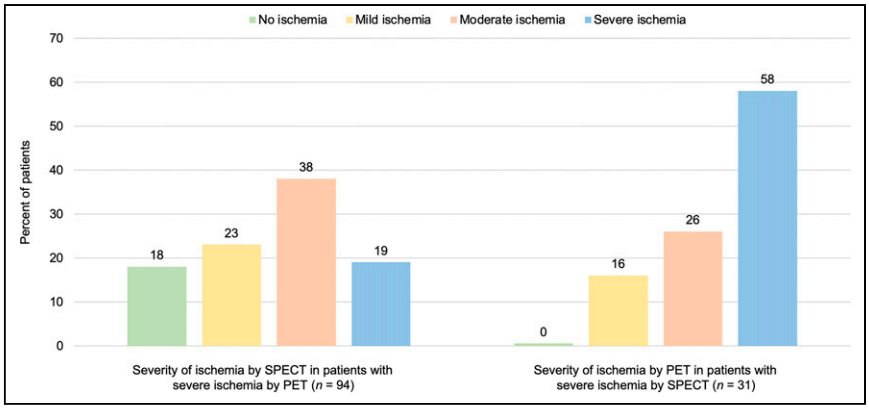

FIGURE 2. Reclassification of severe ischemia by automated perfusion assessment between PET and SPECT MPI (*24*). Among patients with severe ischemia by PET, 41% had either no or mild ischemia when myocardial perfusion was measured via SPECT. Conversely, among patients with severe ischemia on SPECT, 42% had less than severe ischemia by PET MPI.

flow-limiting CAD by avoiding the pitfalls of spatially relative perfusion assessment associated with balanced reduction in myocardial perfusion. In so doing, they improve the sensitivity and negative predictive value of PET MPI for ruling out high-risk angiographic CAD (*28–32*). Indeed, an MFR of more than 2.0 is associated with a negative predictive value of greater than 97% for ruling out high-risk angiographic CAD (*31*). Conversely, normal augmentation in stress MBF and flow reserve in symptomatic patients helps to confidently exclude obstructive CAD and CMD as the potential source of symptoms (*33*), even in the presence of extensive atherosclerosis. From a management perspective, normal stress MBF and flow reserve help avoid the need to pursue coronary angiography.

Quantification of MBF and MFR also provides a powerful tool for incremental risk stratification and risk reclassification. Growing evidence from multiple single-center studies has demonstrated that a preserved flow reserve (>2.0) consistently associates with a low risk of adverse cardiac events, including cardiac death (*34–38*). In contrast, a severe reduction in MFR consistently identifies patients at high risk of adverse cardiac events, even among those with normal findings on myocardial perfusion images. For any amount of ischemic or scarred myocardium, a severely reduced global MFR is associated with a higher risk of death than in the setting of a relatively preserved flow reserve (Fig. 3) (*36–38*). PET measures of MFR improved risk stratification beyond comprehensive clinical assessment, left ventricular ejection fraction, and semiquantitative measures of myocardial ischemia and scarring, and in one study this led to clinically meaningful risk reclassification in about 50% of intermediate-risk patients (*36*). Importantly, stress MBF and flow reserve measurements provide robust complementary information that helps inform clinical risk and subsequent patient management.

The integration of stress MBF and MFR provides a practical way to group individual patients into well-defined risk categories (Fig. 4), thereby facilitating clinical decision-making (*35*). Concordant abnormal stress MBF and MFR identifies the highest-risk patients (cardiac mortality > 3%/y), whereas patients with concordant normal results have the lowest risk (cardiac mortality < 0.5%/y). Discordantly low stress MBF (<1.8) with preserved MFR (>2.0) identifies patients (predominantly male) with epicardial atherosclerosis who have a low risk of adverse events (<1%/y) and in whom revascularization is unlikely to offer a prognostic advantage. Finally, discordantly low MFR (<2.0) with relatively preserved stress MBF (>1.8) identifies patients (predominantly women) without flow-limiting CAD but with an intermediate risk of cardiac death (1.7%/y). This last group with discordant stress MBF and MFR illustrates the clinical advantages to integrating both measurements with respect to diagnosis of obstructive versus nonobstructive CAD and prognostic assessments. For example, what do we do with a patient who has relatively normal stress MBF but reduced MFR and visually normal perfusion? Does the low MFR imply the presence of balanced multivessel obstructive CAD? In this group of patients, the normal stress MBF excludes flow-limiting CAD with high confidence (*28*,*29*,*31*,*32*) whereas the reduced MFR identifies increased risk of adverse cardiovascular events.

There is also evidence that the quantitative blood flow information, a measure of coronary vascular health, helps with risk reclassification of patients with cardiometabolic disease. For example, patients with diabetes without known CAD but abnormal MFR had a cardiac mortality risk comparable to that in nondiabetics with known CAD (*25*). Conversely, diabetics without overt CAD with relatively preserved

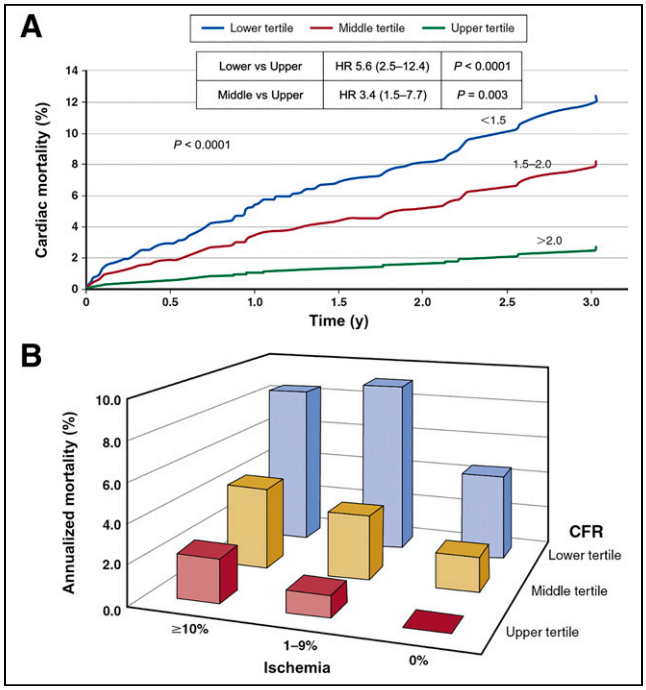

FIGURE 3. (Top) Cumulative adjusted incidence of cardiac mortality for tertiles of coronary flow reserve presented in Kaplan–Meier format showing significant association between coronary flow reserve and cardiac mortality. (Bottom) Unadjusted annualized cardiac mortality by tertiles of coronary flow reserve and categories of myocardial ischemia. Annual rate of cardiac death increased with increasing summed difference score and decreasing coronary flow reserve. Importantly, lower coronary flow reserve consistently identified higher-risk patients at every level of myocardial ischemia, including among those with visually normal PET scans and normal left ventricular function. CFR = coronary flow reserve; HR = hazard ratio. (Reprinted with permission of (*36*).)

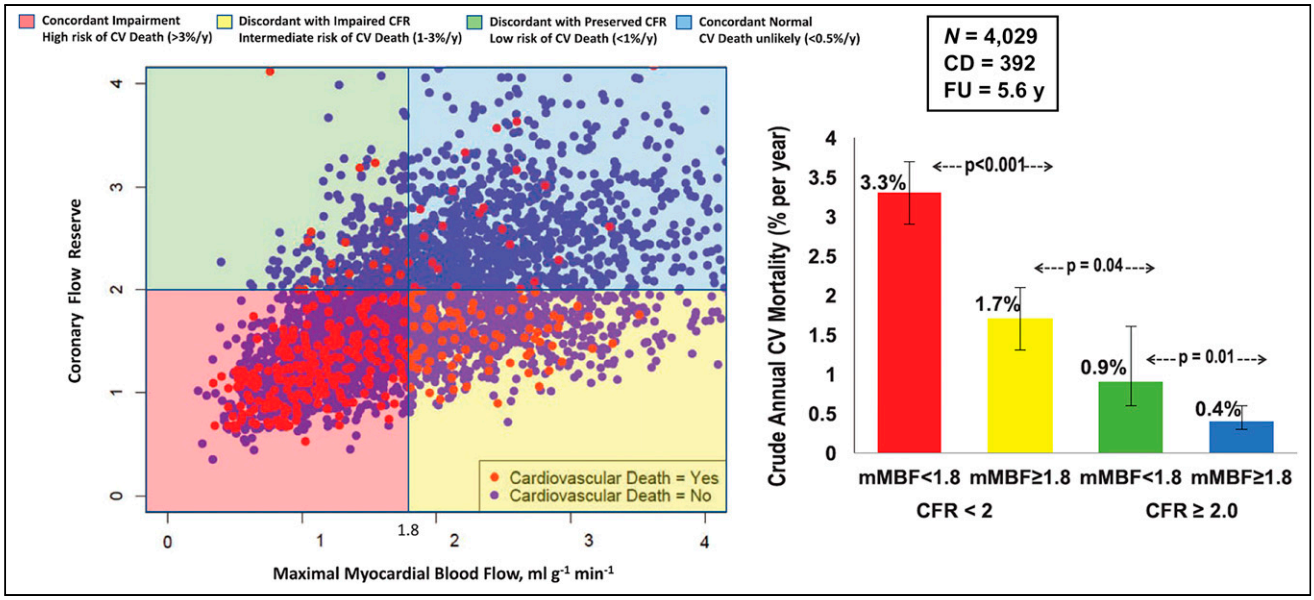

FIGURE 4. (Left) Scatterplot of coronary flow reserve and maximal MBF by cardiovascular death. Concordant and discordant impairment of coronary flow reserve and maximal MBF identifies unique prognostic phenotypes of patients. Coronary flow reserve < 2 and maximal MBF < 1.8 mL·g^{-1}·min^{-1} were defined as impaired. (Right) Unadjusted annualized cardiovascular mortality for 4 groups based on concordant or discordant impairment of CFR and maximal MBF. CD = cardiac death; CFR = coronary flow reserve; CV = cardiovascular; FU = follow-up; mMBF = maximal MBF. (Reprinted with permission of (*35*).)

MFR had an annual risk of less than 1%, which was comparable to subjects without diabetes or CAD.

Given the discussion above, the future efficacy of SPECT MPI will be somewhat tied to its ability to provide routine measurements of MBF. There is growing evidence that SPECT MPI may also provide accurate and reproducible measurements of MBF (*39*–*42*). Although these results are encouraging, quantification of MBF by SPECT requires specialized γ-cameras that provide the necessary high sensitivity and temporal resolution required to enhance the fidelity of flow measurements. Additional challenges include the limitations of the available SPECT perfusion tracers with respect to the extraction roll-off at high flow rates and technical issues with handling increased scatter from subdiaphragmatic activity. Future studies will have to determine their efficacy to enhance diagnosis and risk stratification in patients with suspected or known CAD. Nonetheless, unit dose distribution of ^{18}F-labeled tracers may soon be available and could accelerate the transition from SPECT to PET MPI and obviate some of the challenges associated with SPECT quantification of MBF. Beyond quantification of myocardial perfusion, PET also allows more accurate tracking of left ventricular ejection fraction at rest and during peak stress, which further enhances detection of CAD and risk stratification (*43*).

EXPANDING APPLICATIONS OF QUANTITATIVE MBF WITH PET

Evaluation of CMD

CMD is quite common in symptomatic patients with risk factors, and the relative frequency and severity of CMD are similar in women and men, but there is a larger number of women with CMD than men (*33*,*44*). When CMD is present, symptomatic patients have a worse prognosis (*33*,*44*). Because CMD is a diffuse process, conventional exercise stress testing and stress imaging tests, such as with echocardiography or SPECT imaging, lack sensitivity and specificity for detecting CMD and thus have a relatively limited role in its diagnosis (Fig. 5). Because the coronary microcirculation is beyond the resolution of invasive or noninvasive coronary angiography, direct interrogation of coronary microvascular function is necessary to establish the diagnosis of CMD. There are several noninvasive and invasive approaches for the evaluation of CMD, each with advantages and limitations. This is a unique application of quantitative PET imaging, which is considered the most accurate and reproducible noninvasive technique to interrogate coronary microcirculatory function (*45*). The diagnosis of CMD is based on the finding of reduced stress MBF and MFR. An MFR of less than 2.0 has been traditionally used for diagnosing CMD in the absence of flow-limiting CAD. However, it is important to keep in mind that MFR declines with age, so a single quantitative threshold may not have the same sensitivity in younger individuals as in older individuals. For example, higher thresholds (e.g., 2.5) have been used in younger women with rheumatoid arthritis and other systemic inflammatory disorders (*46*–*49*). Nonetheless, an MFR of less than 2.0 consistently identifies patients at higher risk of adverse events (*22*,*33*,*44*,*49*). The presence of diffuse nonobstructive atherosclerosis in the epicardial coronary arteries is a common finding in most symptomatic patients with CMD. Thus, the reduction of stress MBF and MFR results from the combined effects of altered coronary fluid dynamics caused by diffuse atherosclerosis and of microcirculatory dysfunction caused by endothelial-cell or smooth muscle–cell abnormalities and contributing to myocardial ischemia and symptoms. The association between extensive nonobstructive atherosclerosis and CMD increased clinical risk compared with either one alone (*45*). This highlights the important complementary role of delineating atherosclerotic burden with CT as discussed below.

Evaluation of Coronary Allograft Vasculopathy

Although cardiac transplantation has improved outcomes in patients with advanced heart failure, cardiac allograft vasculopathy remains a leading cause of mortality and retransplantation in these individuals. Because of myocardial denervation, silent ischemia

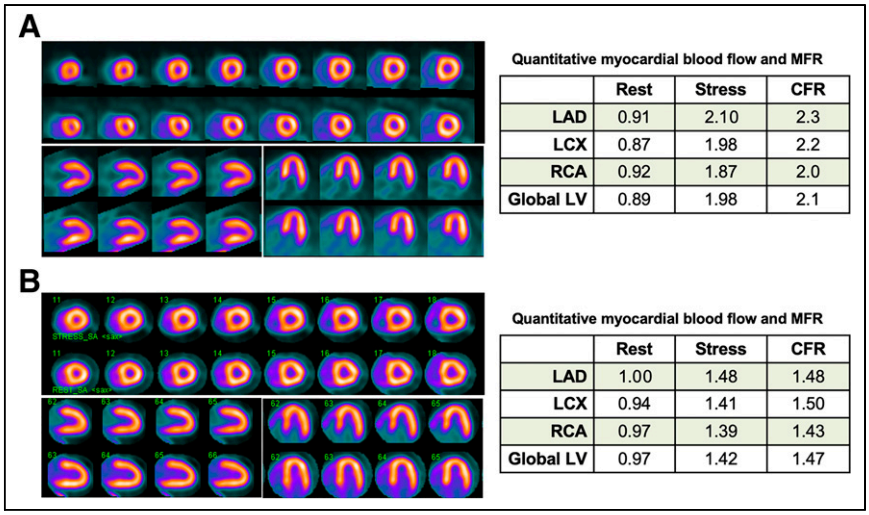

FIGURE 5. Examples of patients with and without CMD. (A) A 58-y-old man with hypertension and diabetes evaluated for atypical chest pain. (B) A 63-y-old man with hypertension, diabetes, and high cholesterol evaluated for dyspnea. In both cases, myocardial perfusion results are normal, suggesting no evidence of flow-limiting CAD. Patient A has normal stress MBF and MFR. However, patient B shows severely reduced stress MBF and MFR. Follow-up CT coronary angiography showed no evidence of obstructive CAD. Thus, abnormalities in coronary vasoreactivity in patient B are consistent with CMD. CFR = coronary flow reserve; LAD = left anterior descending coronary artery; LCX = left circumflex coronary artery; LV = left ventricular; RCA = right coronary artery.

is common. Annual surveillance with invasive angiography, endomyocardial biopsy, and imaging is routine in these patients. Transplant vasculopathy develops as diffuse disease that may not result in discrete perfusion defects on MPI. Emerging data from multiple centers have provided evidence that cardiac PET–measured MBF is a sensitive tool with a high negative predictive value to rule out cardiac allograft vasculopathy (*50–54*). Moreover, patients with PET-defined vasculopathy are at significantly higher risk of mortality (*50–54*). Indeed, in patients with serial PET assessments, patients with a decline in MBF had worse prognosis (*53*).

INTEGRATING CT TO AUGMENT VALUE OF MPI WITH HYBRID PET/CT

Over the last 20 y, there has been increasing recognition of the value of atherosclerotic burden in the identification of patients with high and low cardiovascular risk. This has led to the hypothesis that integrated assessment of the anatomic burden of disease via CT and its functional significance with radionuclide MPI using hybrid imaging (SPECT/CT and PET/CT) can enhance diagnosis and risk prediction, thereby opening new opportunities to improve patient outcomes. The extent and severity of CAC by CT reflects the burden of atherosclerosis in the coronary arteries and can be quantified by validated scoring techniques (e.g., Agatston score). A score of 0 indicates no coronary calcification and portends a very low risk of adverse cardiovascular events, whereas a score greater than 0 indicates the presence of mild, moderate, or severe calcification and a higher clinical risk (*55*). The integration of CAC with SPECT and PET MPI can improve the diagnostic performance of radionuclide MPI (*56*,*57*) and provides complementary risk stratification (Fig. 6) (*27*,*58–63*). Given the clinical relevance of atherosclerotic burden assessment in guiding initiation and intensification of preventive therapies (*64*,*65*), a formal or semiquantitative CAC score should be assessed and reported in all patients without known CAD undergoing myocardial perfusion PET/CT imaging as it provides actionable clinical information. The nongated CT transmission scan used for attenuation correction of the PET data may also be used to assess the extent of coronary calcifications using semiquantitative visual analysis (*66*,*67*). Artificial intelligence techniques can now facilitate the extraction of quantitative CAC estimates from these ungated CT maps obtained during cardiac PET/CT imaging without the need of the added radiation from the gated calcium scan (Fig. 7) (*60*,*68–70*).

There is also evidence that quantification of MBF further enhances the clinical value of hybrid imaging. There is a modest stepwise increase in the frequency of abnormal MFR with increasing CAC scores, especially in the absence of focal obstructive CAD (*58*,*62*). In this context, the modest reduction in MFR reflects the integrated fluid dynamic effects of diffuse large-vessel atherosclerosis and microcirculatory dysfunction. Consequently, the quantitative flow measurement is a useful surrogate marker of disease activity in the coronary circulation that may reflect active pathophysiologic changes, which are more readily reversible with medical and lifestyle interventions than coronary calcifications. The scatter of coronary vasodilator reserve values in each CAC score category suggests that calcium deposits are not a complete reflection of overall disease activity within the coronary circulation (*62*). A key concept borne out from previous studies (*58*,*62*) is that relatively preserved vascular health as assessed by MFR consistently identifies lower-risk patients at any strata of CAC, which may help explain the relatively low numbers of coronary events even among patients with high coronary artery calcium

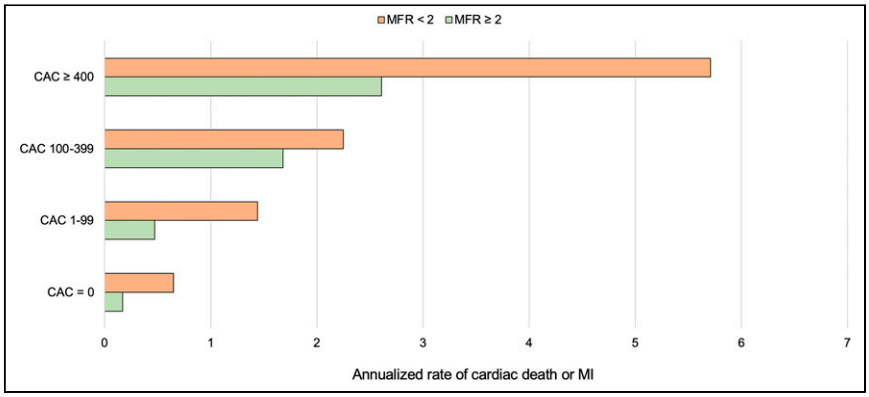

FIGURE 6. Unadjusted annualized rate of cardiac death and nonfatal myocardial infarction by coronary artery calcium score and myocardial flow reserve category. At every calcium score stratum, there is increased rate of adverse events with reduced myocardial flow reserve. MI = myocardial infarction. (Reprinted with permission of (*58*).)

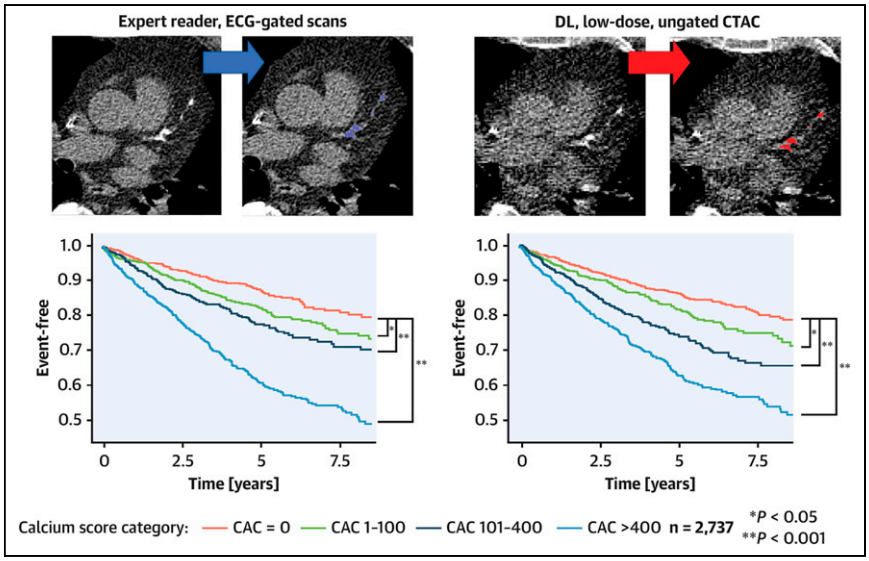

FIGURE 7. Comparison of outcomes by expert reader standard CAC score from electrocardiography-gated CT vs. score calculated automatically by deep learning from PET/CT attenuation correction maps. (Top) Kaplan–Meier curves for major adverse cardiac event risk by coronary artery calcium score categories. (Bottom) Univariate major adverse cardiac event risk analysis using proportional-hazards Cox model. CAC = coronary artery calcium; CTAC = CT attenuation correction; DL = deep learning; ECG = electrocardiography. (Reprinted with permission of (*70*).)

scores (*55*). Thus, both CAC and flow quantification may help inform the intensity of preventive therapies.

EXPANDING ACCESS TO RADIONUCLIDE PERFUSION IMAGING WITH PET

Over the last decade, there has been a steady shift from SPECT to PET/CT MPI in the United States. This shift is likely multifactorial, including the mounting evidence for the superior diagnostic accuracy and incremental risk stratification of PET/CT over SPECT in the evaluation of CAD. However, access to cardiac PET is significantly more limited than to SPECT, in part related to the availability of radiopharmaceuticals for MPI. Although access to ^{82}Sr/^{82}Rb generators and regional medical cyclotrons dedicated to ^{13}N-ammonia production has enabled significant growth in cardiac PET/CT, this remains costly and likely a viable option only for relatively high-volume centers. The recent successful completion of phase III trials for ^{18}F-flurpiridaz (*71*) and its expected Food and Drug Administration approval will enable unit dose radiotracer distribution from commercial radiopharmacies, which will likely help reduce overall costs and expand access to cardiac PET within and outside the United States. In addition, ^{15}O-water is currently undergoing phase III evaluation in an international clinical trial and may add powerful options for clinical PET MPI (NCT05134012).

CONCLUSION

Radionuclide MPI has played a transformative role in the management of patients with CAD for the last 50 y. However, the emergence of new alternative technologies and the changes in CAD presentations with a rise in diffuse nonobstructive CAD and coronary microcirculatory dysfunction require a recalibration of our toolbox to provide effective answers to these challenges. The integration of MBF quantification by PET, and potentially SPECT, and assessment of CAC provides the key that offers unique and complementary diagnostic and prognostic information across the spectrum of CAD risk. The expected growth of radiopharmaceutical options for PET in the near future promises to rapidly expand access to and likely reduce the costs of PET MPI. Many of the challenging quantitative tasks will continue to be simplified and automated by artificial intelligence. This opens an exciting future for cardiovascular nuclear medicine to maintain and expand its transformative role in patient care and research.

DISCLOSURE

Marcelo Di Carli is supported by grants from the NIH (R01HL162960 and R01EB034586). He also received an institutional research grant from Gilead Sciences; consulting honoraria from Sanofi, MedTrace Pharma, and Valo Health; and in-kind research support from Amgen. No other potential conflict of interest relevant to this article was reported.

REFERENCES

1. Zaret BL, Strauss HW, Hurley PJ, Natarajan TK, Pitt B. A noninvasive scintiphotographic method for detecting regional ventricular dysfunction in man. *N Engl J Med.* 1971;284:1165–1170.
2. Shaw LJ, Hage FG, Berman DS, Hachamovitch R, Iskandrian A. Prognosis in the era of comparative effectiveness research: where is nuclear cardiology now and where should it be? *J Nucl Cardiol.* 2012;19:1026–1043.
3. Dorbala S, Di Carli MF, Beanlands RS, et al. Prognostic value of stress myocardial perfusion positron emission tomography: results from a multicenter observational registry. *J Am Coll Cardiol.* 2013;61:176–184.
4. Han D, Rozanski A, Gransar H, et al. Myocardial ischemic burden and differences in prognosis among patients with and without diabetes: results from the multicenter international REFINE SPECT registry. *Diabetes Care.* 2020;43:453–459.
5. Al-Mallah MH, Hachamovitch R, Dorbala S, Di Carli MF. Incremental prognostic value of myocardial perfusion imaging in patients referred to stress single-photon emission computed tomography with renal dysfunction. *Circ Cardiovasc Imaging.* 2009;2:429–436.
6. Jespersen L, Hvelplund A, Abildstrom SZ, et al. Stable angina pectoris with no obstructive coronary artery disease is associated with increased risks of major adverse cardiovascular events. *Eur Heart J.* 2012;33:734–744.
7. Maddox TM, Stanislawski MA, Grunwald GK, et al. Nonobstructive coronary artery disease and risk of myocardial infarction. *JAMA.* 2014;312:1754–1763.
8. Patel MR, Dai D, Hernandez AF, et al. Prevalence and predictors of nonobstructive coronary artery disease identified with coronary angiography in contemporary clinical practice. *Am Heart J.* 2014;167:846–52.e2.
9. Gerber Y, Gibbons RJ, Weston SA, et al. Coronary disease surveillance in the community: angiography and revascularization. *J Am Heart Assoc.* 2020;9:e015231.
10. Jouni H, Askew JW, Crusan DJ, Miller TD, Gibbons RJ. Temporal trends of single-photon emission computed tomography myocardial perfusion imaging in patients with coronary artery disease: a 22-year experience from a tertiary academic medical center. *Circ Cardiovasc Imaging.* 2017;10:e005628.
11. Rozanski A, Gransar H, Hayes SW, et al. Temporal trends in the frequency of inducible myocardial ischemia during cardiac stress testing: 1991 to 2009. *J Am Coll Cardiol.* 2013;61:1054–1065.
12. Neumann JT, Gossling A, Sorensen NA, Blankenberg S, Magnussen C, Westermann D. Temporal trends in incidence and outcome of acute coronary syndrome. *Clin Res Cardiol.* 2020;109:1186–1192.
13. Yeh RW, Sidney S, Chandra M, Sorel M, Selby JV, Go AS. Population trends in the incidence and outcomes of acute myocardial infarction. *N Engl J Med.* 2010;362:2155–2165.

14. Tsao CW, Aday AW, Almarzooq ZI, et al. Heart disease and stroke statistics: 2023 update—a report from the American Heart Association. *Circulation.* 2023;147: e93–e621.
15. Roberts WC. Quantitative extent of atherosclerotic plaque in the major epicardial coronary arteries in patients with fatal coronary heart disease, in coronary endarterectomy specimens, in aorta-coronary saphenous venous conduits, and means to prevent the plaques: a review after studying the coronary arteries for 50 years. *Am J Cardiol.* 2018;121:1413–1435.
16. Taube A, Schlich R, Sell H, Eckardt K, Eckel J. Inflammation and metabolic dysfunction: links to cardiovascular diseases. *Am J Physiol Heart Circ Physiol.* 2012; 302:H2148–H2165.
17. Kalogeropoulos A, Georgiopoulou V, Psaty BM, et al. Inflammatory markers and incident heart failure risk in older adults: the Health ABC (Health, Aging, and Body Composition) study. *J Am Coll Cardiol.* 2010;55:2129–2137.
18. Taqueti VR, Shah AM, Everett BM, et al. Coronary flow reserve, inflammation, and myocardial strain: the CIRT-CFR trial. *JACC Basic Transl Sci.* 2022;8: 141–151.
19. Bajaj NS, Singh A, Zhou W, et al. Coronary microvascular dysfunction, left ventricular remodeling, and clinical outcomes in patients with chronic kidney impairment. *Circulation.* 2020;141:21–33.
20. Brown JM, Zhou W, Weber B, et al. Low coronary flow relative to myocardial mass predicts heart failure in symptomatic hypertensive patients with no obstructive coronary artery disease. *Eur Heart J.* 2022;43:3323–3331.
21. Taqueti VR, Solomon SD, Shah AM, et al. Coronary microvascular dysfunction and future risk of heart failure with preserved ejection fraction. *Eur Heart J.* 2018; 39:840–849.
22. Zhou W, Brown JM, Bajaj NS, et al. Hypertensive coronary microvascular dysfunction: a subclinical marker of end organ damage and heart failure. *Eur Heart J.* 2020;41:2366–2375.
23. Murthy VL, Naya M, Foster CR, et al. Coronary vascular dysfunction and prognosis in patients with chronic kidney disease. *JACC Cardiovasc Imaging.* 2012;5: 1025–1034.
24. Patel FS, Bateman TM, Spertus JA, et al. Reclassification of severe ischemia on PET versus SPECT MPI using a same-patient simultaneous imaging protocol. *JACC Cardiovasc Imaging.* 2022;15:1158–1159.
25. Murthy VL, Naya M, Foster CR, et al. Association between coronary vascular dysfunction and cardiac mortality in patients with and without diabetes mellitus. *Circulation.* 2012;126:1858–1868.
26. Charytan DM, Skali H, Shah NR, et al. Coronary flow reserve is predictive of the risk of cardiovascular death regardless of chronic kidney disease stage. *Kidney Int.* 2018;93:501–509.
27. Patel KK, Peri-Okonny PA, Qarajeh R, et al. Prognostic relationship between coronary artery calcium score, perfusion defects, and myocardial blood flow reserve in patients with suspected coronary artery disease. *Circ Cardiovasc Imaging.* 2022; 15:e012599.
28. Danad I, Raijmakers PG, Driessen RS, et al. Comparison of coronary CT angiography, SPECT, PET, and hybrid imaging for diagnosis of ischemic heart disease determined by fractional flow reserve. *JAMA Cardiol.* 2017;2:1100–1107.
29. Danad I, Uusitalo V, Kero T, et al. Quantitative assessment of myocardial perfusion in the detection of significant coronary artery disease: cutoff values and diagnostic accuracy of quantitative [^{15}O]H_2O PET imaging. *J Am Coll Cardiol.* 2014; 64:1464–1475.
30. Kajander S, Joutsiniemi E, Saraste M, et al. Cardiac positron emission tomography/computed tomography imaging accurately detects anatomically and functionally significant coronary artery disease. *Circulation.* 2010;122:603–613.
31. Naya M, Murthy VL, Taqueti VR, et al. Preserved coronary flow reserve effectively excludes high-risk coronary artery disease on angiography. *J Nucl Med.* 2014;55:248–255.
32. Ziadi MC, Dekemp RA, Williams K, et al. Does quantification of myocardial flow reserve using rubidium-82 positron emission tomography facilitate detection of multivessel coronary artery disease? *J Nucl Cardiol.* 2012;19:670–680.
33. Murthy VL, Naya M, Taqueti VR, et al. Effects of sex on coronary microvascular dysfunction and cardiac outcomes. *Circulation.* 2014;129:2518–2527.
34. Gould KL, Kitkungvan D, Johnson NP, et al. Mortality prediction by quantitative PET perfusion expressed as coronary flow capacity with and without revascularization. *JACC Cardiovasc Imaging.* 2021;14:1020–1034.
35. Gupta A, Taqueti VR, van de Hoef TP, et al. Integrated noninvasive physiological assessment of coronary circulatory function and impact on cardiovascular mortality in patients with stable coronary artery disease. *Circulation.* 2017;136: 2325–2336.
36. Murthy VL, Naya M, Foster CR, et al. Improved cardiac risk assessment with noninvasive measures of coronary flow reserve. *Circulation.* 2011;124:2215–2224.
37. Patel KK, Spertus JA, Chan PS, et al. Myocardial blood flow reserve assessed by positron emission tomography myocardial perfusion imaging identifies patients with a survival benefit from early revascularization. *Eur Heart J.* 2020;41: 759–768.
38. Ziadi MC, Dekemp RA, Williams KA, et al. Impaired myocardial flow reserve on rubidium-82 positron emission tomography imaging predicts adverse outcomes in patients assessed for myocardial ischemia. *J Am Coll Cardiol.* 2011;58:740–748.
39. Agostini D, Roule V, Nganoa C, et al. First validation of myocardial flow reserve assessed by dynamic ^{99m}Tc-sestamibi CZT-SPECT camera: head to head comparison with ^{15}O-water PET and fractional flow reserve in patients with suspected coronary artery disease. The WATERDAY study. *Eur J Nucl Med Mol Imaging.* 2018;45:1079–1090.
40. Ben Bouallègue F, Roubille F, Lattuca B, et al. SPECT myocardial perfusion reserve in patients with multivessel coronary disease: correlation with angiographic findings and invasive fractional flow reserve measurements. *J Nucl Med.* 2015;56: 1712–1717.
41. Ben-Haim S, Murthy VL, Breault C, et al. Quantification of myocardial perfusion reserve using dynamic SPECT imaging in humans: a feasibility study. *J Nucl Med.* 2013;54:873–879.
42. de Souza AC, Harms HJ, Martell L, et al. Accuracy and reproducibility of myocardial blood flow quantification by single photon emission computed tomography imaging in patients with known or suspected coronary artery disease. *Circ Cardiovasc Imaging.* 2022;15:e013987.
43. Dorbala S, Vangala D, Sampson U, Limaye A, Kwong R, Di Carli MF. Value of vasodilator left ventricular ejection fraction reserve in evaluating the magnitude of myocardium at risk and the extent of angiographic coronary artery disease: a ^{82}Rb PET/CT study. *J Nucl Med.* 2007;48:349–358.
44. Patel KK, Shaw L, Spertus JA, et al. Association of sex, reduced myocardial flow reserve, and long-term mortality across spectrum of atherosclerotic disease. *JACC Cardiovasc Imaging.* 2022;15:1635–1644.
45. Taqueti VR, Di Carli MF. Coronary microvascular disease pathogenic mechanisms and therapeutic options: JACC state-of-the-art review. *J Am Coll Cardiol.* 2018;72: 2625–2641.
46. Amigues I, Russo C, Giles JT, et al. Myocardial microvascular dysfunction in rheumatoid arthritis: quantitation by ^{13}N-ammonia positron emission tomography/computed tomography. *Circ Cardiovasc Imaging.* 2019;12:e007495.
47. Feher A, Boutagy NE, Oikonomou EK, et al. Association between impaired myocardial flow reserve on ^{82}rubidium positron emission tomography imaging and adverse events in patients with autoimmune rheumatic disease. *Circ Cardiovasc Imaging.* 2021;14:e012208.
48. Weber BN, Stevens E, Barrett L, et al. Coronary microvascular dysfunction in systemic lupus erythematosus. *J Am Heart Assoc.* 2021;10:e018555.
49. Weber BN, Stevens E, Perez-Chada LM, et al. Impaired coronary vasodilator reserve and adverse prognosis in patients with systemic inflammatory disorders. *JACC Cardiovasc Imaging.* 2021;14:2212–2220.
50. Bravo PE, Bergmark BA, Vita T, et al. Diagnostic and prognostic value of myocardial blood flow quantification as non-invasive indicator of cardiac allograft vasculopathy. *Eur Heart J.* 2018;39:316–323.
51. Chih S, Chong AY, Bernick J, et al. Validation of multiparametric rubidium-82 PET myocardial blood flow quantification for cardiac allograft vasculopathy surveillance. *J Nucl Cardiol.* 2021;28:2286–2298.
52. Chih S, Chong AY, Dzavik V, et al. Fibrotic plaque and microvascular dysfunction predict early cardiac allograft vasculopathy progression after heart transplantation: the early post transplant cardiac allograft vasculopathy study. *Circ Heart Fail.* 2023;16:e010173.
53. Feher A, Srivastava A, Quail MA, et al. Serial assessment of coronary flow reserve by rubidium-82 positron emission tomography predicts mortality in heart transplant recipients. *JACC Cardiovasc Imaging.* 2020;13:109–120.
54. Mc Ardle BA, Davies RA, Chen L, et al. Prognostic value of rubidium-82 positron emission tomography in patients after heart transplant. *Circ Cardiovasc Imaging.* 2014;7:930–937.
55. Detrano R, Guerci AD, Carr JJ, et al. Coronary calcium as a predictor of coronary events in four racial or ethnic groups. *N Engl J Med.* 2008;358:1336–1345.
56. Brodov Y, Gransar H, Dey D, et al. Combined quantitative assessment of myocardial perfusion and coronary artery calcium score by hybrid ^{82}Rb PET/CT improves detection of coronary artery disease. *J Nucl Med.* 2015;56:1345–1350.
57. Zampella E, Acampa W, Assante R, et al. Combined evaluation of regional coronary artery calcium and myocardial perfusion by ^{82}Rb PET/CT in the identification of obstructive coronary artery disease. *Eur J Nucl Med Mol Imaging.* 2018;45: 521–529.
58. Aljizeeri A, Ahmed AI, Alfaris MA, et al. Myocardial flow reserve and coronary calcification in prognosis of patients with suspected coronary artery disease. *JACC Cardiovasc Imaging.* 2021;14:2443–2452.

59. Chang SM, Nabi F, Xu J, et al. The coronary artery calcium score and stress myocardial perfusion imaging provide independent and complementary prediction of cardiac risk. *J Am Coll Cardiol.* 2009;54:1872–1882.
60. Feher A, Pieszko K, Miller R, et al. Integration of coronary artery calcium scoring from CT attenuation scans by machine learning improves prediction of adverse cardiovascular events in patients undergoing SPECT/CT myocardial perfusion imaging. *J Nucl Cardiol.* 2023;30:590–603.
61. Miller RJH, Han D, Singh A, et al. Relationship between ischaemia, coronary artery calcium scores, and major adverse cardiovascular events. *Eur Heart J Cardiovasc Imaging.* 2022;23:1423–1433.
62. Naya M, Murthy VL, Foster CR, et al. Prognostic interplay of coronary artery calcification and underlying vascular dysfunction in patients with suspected coronary artery disease. *J Am Coll Cardiol.* 2013;61:2098–2106.
63. Schenker MP, Dorbala S, Hong EC, et al. Interrelation of coronary calcification, myocardial ischemia, and outcomes in patients with intermediate likelihood of coronary artery disease: a combined positron emission tomography/computed tomography study. *Circulation.* 2008;117:1693–1700.
64. Gupta A, Lau E, Varshney R, et al. The identification of calcified coronary plaque is associated with initiation and continuation of pharmacological and lifestyle preventive therapies: a systematic review and meta-analysis. *JACC Cardiovasc Imaging.* 2017;10:833–842.
65. SCOT-HEART Investigators; Newby DE, Adamson PD, et al. Coronary CT angiography and 5-year risk of myocardial infarction. *N Engl J Med.* 2018;379:924–933.
66. Einstein AJ, Johnson LL, Bokhari S, et al. Agreement of visual estimation of coronary artery calcium from low-dose CT attenuation correction scans in hybrid PET/CT and SPECT/CT with standard Agatston score. *J Am Coll Cardiol.* 2010; 56:1914–1921.
67. Pieszko K, Shanbhag AD, Lemley M, et al. Reproducibility of quantitative coronary calcium scoring from PET/CT attenuation maps: comparison to ECG-gated CT scans. *Eur J Nucl Med Mol Imaging.* 2022;49:4122–4132.
68. Išgum I, de Vos BD, Wolterink JM, et al. Automatic determination of cardiovascular risk by CT attenuation correction maps in Rb-82 PET/CT. *J Nucl Cardiol.* 2018;25:2133–2142.
69. Lessmann N, van Ginneken B, Zreik M, et al. Automatic calcium scoring in low-dose chest CT using deep neural networks with dilated convolutions. *IEEE Trans Med Imaging.* 2018;37:615–625.
70. Pieszko K, Shanbhag A, Killekar A, et al. Deep learning of coronary calcium scores from PET/CT attenuation maps accurately predicts adverse cardiovascular events. *JACC Cardiovasc Imaging.* 2023;16:675–687.
71. Maddahi J, Lazewatsky J, Udelson JE, et al. Phase-III clinical trial of fluorine-18 flurpiridaz positron emission tomography for evaluation of coronary artery disease. *J Am Coll Cardiol.* 2020;76:391–401.